Simulation and reduction of radar cross section the unmanned aerial vehicle in X-band using Shaping technique

Hamid Heidar[1], Naser Moradisoltani[2], Omid Alihemati[3]
1- Department of Electronics and Communication, Malek-Ashtar University of Technology, Tehran , Iran, hheidar@aut.ac.ir
2- Department of Electronics and Communication, Malek-Ashtar University of Technology, Tehran, Iran, Nasser_soltani35@yahoo.com
3- Department of Materials, Malek-Ashtar University of Technology, Tehran , Iran, oah65_2005@yahoo.com

Received: August 20, 2012 Revised: September 11, 2012 Accepted: September 25, 2012

ABSTRACT:
Radar Cross Section (RCS) reduction is very important factor to increase survivability. This paper used a model of the Unmanned Aerial Vehicle (UAV) will be as a reference and focus on RCS reduction by using shaping methods. Simulation software CST was used to calculate the RCS of aerial targets. Four types of target geometries are simulated to find the final optimal design which will give a less value of RCS compared with the reference geometry over X-Band (8, 9,10,11,12 GHz are used for simulation then average value is drowned).

KEYWORDS: Radar Cross Section; Unmanned Aerial Vehicle; Shaping Technique; Simulation software CST; Asymptotic solver; Radar Cross Section Average; nose; wing; tail.

1. INTRODUCTION

Calculation of RCS is essentially a matter of finding the scattered electric field from a target. If the current induced on the target by the incident plane wave can be determined, the same radiation integrals used in antenna analysis can be applied to compute the scattered field [1]. The computation of RCS over an aerial target is arising from different mechanisms, such as specular reflection, diffraction, creeping wave, and multiple scattering. The contribution of each of these mechanisms varies with the target geometry and material composition, angular orientation of target relative to transmitter and receiver, frequency or wavelength and transmitter polarization [2].

Radar cross section diagrams are usually difficult to interpret because they are two-dimensional representations of three-dimensional objects. Moreover, the difficulties in interpreting RCS diagrams are dependent upon the geometry of the object and sometimes, on the techniques used to calculate the RCS [4].

In this paper four targets are simulated over X-band, these targets are:

i. Target geometry 1: it consists of a model Unmanned Aerial Vehicle built as a reference, regardless of the simulation engine.

ii. Target geometry 2: it consists of nose. One of nose (tangent ogive in four types) reference body geometry 1 without wings and tail was selected and simulated, and then by depending on RCS results one of these noses was used to build the geometry3.

iii. Target geometry 3: it consists of Target geometry2 and wing. Three types of wings (delta) and one type of position on the body of target were selected and simulated. The best geometry which gave less RCS value was used to build the geometr3

iiii. Target geometry 4: it consists of Target geometry4 and tail. Three types of tails were selected and simulated and this is final geometry.

To give our results credibility, three of the final and reference geometries was simulated and their difference is in wing and tail, the area for all wings type and tails type will be equal.

2. RADAR CROSS SECTION

The RCS of an object is a direct measure of its visibility to radar. The RCS can be defined as the area of a fictitious perfect reflector of electromagnetic waves that would reflect the same amount of energy back to the transmitting/receiving radar antenna, as would the actual target [10]. The RCS is dependent on the radar wavelength and polarization, aspect angle, shape and target material properties. It is referred to as monostatic when the transmitter and receiver are in the same location. The monostatic RCS, in terms of electric field, is given by [9]

$$\pm = \lim_{\to\infty} 4\circledR r^2 \frac{\left|E_s\right|^2}{\left|E_I\right|^2} \quad (1)$$

Where, r is the distance from the target to the radar, E_S and E_I are the scattered and incident electric fields, respectively. Equation (1) is valid when the target is illuminated by a plane wave. This is satisfied by the

far-field approximation, i.e., when the object is located at a distance at least $r = \frac{2D^2}{a}$ where D is the largest dimension of the object. Due to the large range of RCS values, a logarithmic power scale is used with the reference value of $\sigma_R = 1\ m^2$ [9]:

$$\pm_L = 10\log_{10}\left(\frac{\pm}{\pm_R}\right) = 10\log_{10}\left(\frac{\pm}{1}\right) \qquad (2)$$

3. SOFTWARE SIMULATION

The software CST was used for simulation because it has hybrid method transient solver (T-solver), integral equation solver (I-solver), which is hybrid between High frequency techniques and Numerical methods [5]. It should be mentioned that all of the RCS data are normalized to the maximum value. High frequency techniques, such as T-solver, I-solver have been successfully applied to RCS modeling in optical region [6]. The main difficulty for RCS prediction of complex targets using high-frequency techniques is computation of surface and line integrals over an arbitrary shape [7].

Numerical methods, such as method of moments I-solver and T-solver techniques are powerful RCS simulators applicable in resonance but these methods need huge RAM for large target over high frequency like X-band, So the Asymptotic solver(A-solver) method that requires less RAM than the T-solver and I-solver are used in this paper.

3.1 Target Geometry 1

Target geometry consists of a model for unmanned aerial vehicle built as the reference geometry is considered. Figure. 1 show target geometry 1.

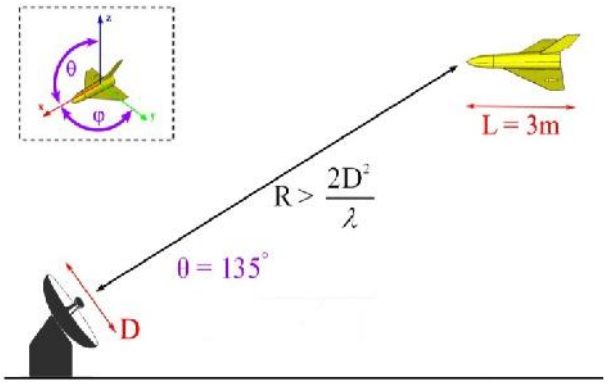

Fig. 1. Target geometry 1

Figure. 2 shows the RCS average value of target geometry1 over X-band .The RCS computations were performed at: $\theta = 135^0$ and $\varphi = 0{:}360^0$ with 1^0 steps.

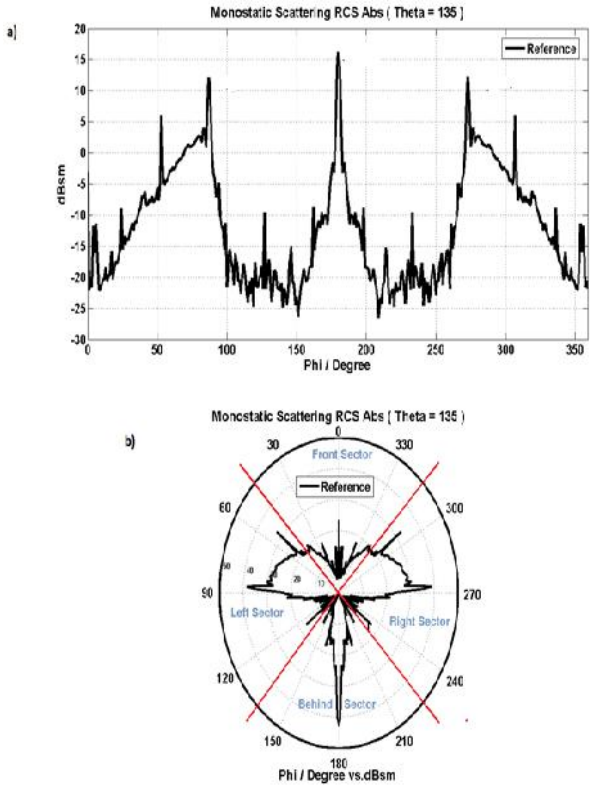

Fig. 2. a) Average value of radar cross section at four angular sectors geometry1 over X-Band, b) Normalized RCS to maximum value (polar mode)

3.2 Target Geometry 2

Target geometry consists of nose. In all of the following nosecone shape equations, ***L*** is the overall length of the nosecone, and ***R*** is the radius of the base of the nosecone [3]. Figure.. 3 show the nose shape.

$$y = \sqrt{\rho^2 - (x-l)^2} + (R-\rho) \quad \text{where } \rho = \frac{R^2 + L^2}{2R} \qquad (3)$$

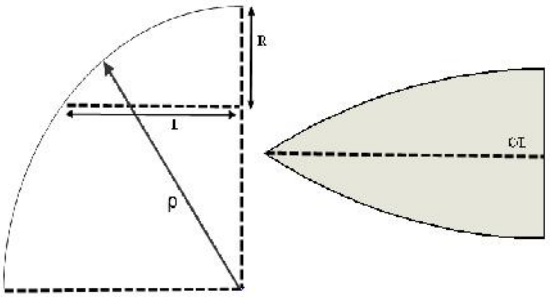

Fig. 3. nose shape(ogive)

Figure. 4 shows three type of model1 the difference between those three types is nose we select Target 2-3.

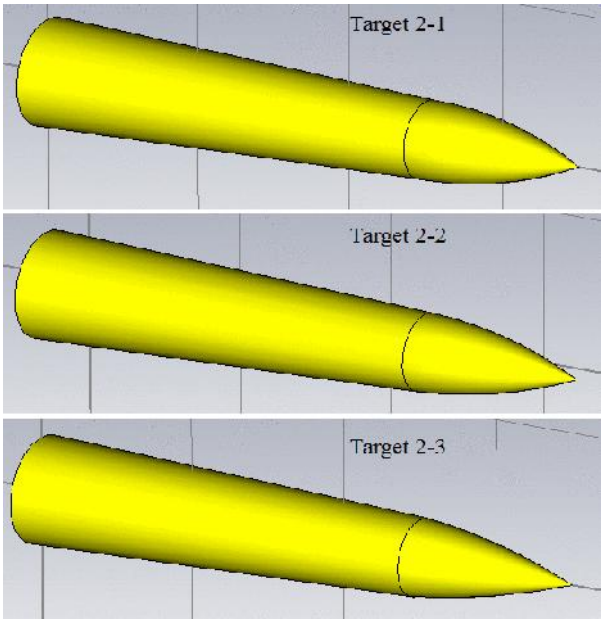

Fig. 4. Target geometry 2

Shows the RCS value of target geometry1 over X-band. The RCS computations were performed at: $\theta = 135^{o}$ and $\varphi = 0{:}360^{0}$ with 1^{0} steps.

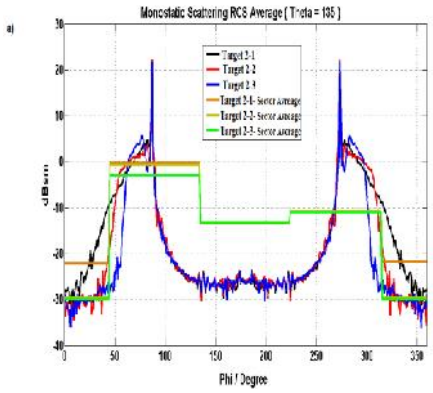

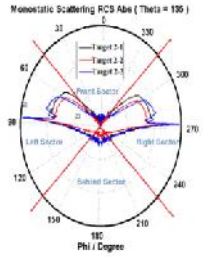

Fig. 5. a) Average value of radar cross section at four angular sectors geometry2 over X-Band, b) Normalized RCS to maximum value (polar mode).

Table 1 shows the RCS average value of geometry2 over X-band and average over four types of target geometries , we can find from Table1, the best average RCS value is by using target 2-3.

Table1: The RCS average value of Geometry1 over X-Band (θ=135^{0})

Geometry2	RCS Average (dBsm) for θ = 135^{0}				
	Total average	**φ = $315{:}45^{0}$ Front sector**	**φ = $45{:}135^{0}$ Left sector**	**φ = $135{:}225^{0}$ Behind sector**	**φ = $225{:}315^{0}$ Right sector**
Target 2-1	**-17.52**	**-22.26**	**-0.37**	**-13.31**	**-11.04**
Target 2-2	**-19.61**	**-29.75**	**-0.65**	**-13.31**	**-11.04**
Target 2-3	**-21.00**	**-30.00**	**-3.07**	**-13.31**	**-11.04**

3.3 Target Geometry 3

Target geometry 3 consist of target geometry 2 and wings. There are three main types of wings: Delta. For comparison, the area for all wings type will be equal. Figure. 6 show those types.

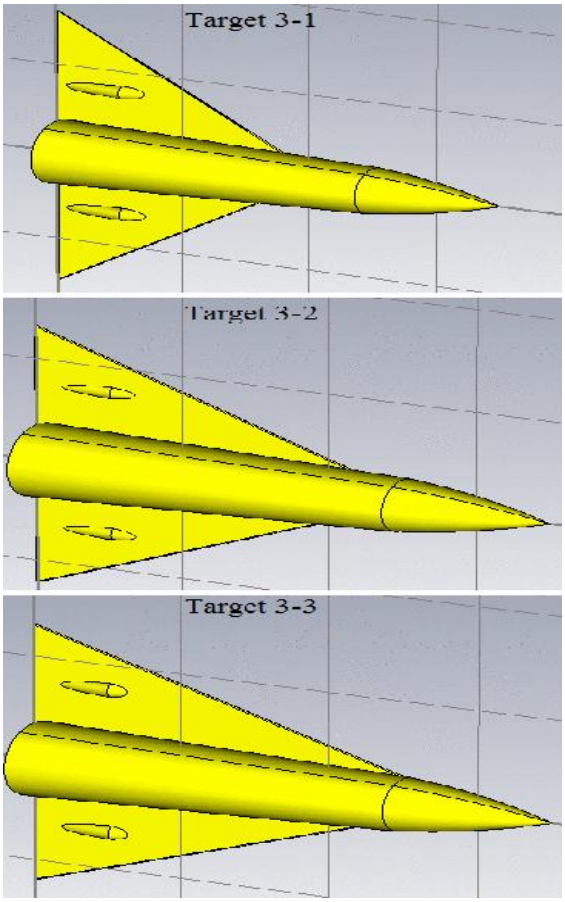

Fig. 6. Target geometry 3

Figure. 7 show consecutively the RCS average value of target geometry3-Delta RCS over X-band. The

RCS computations were performed at: $\theta = 135^0$ and

$\varphi = 0{:}360^0$ with 1^0 steps.

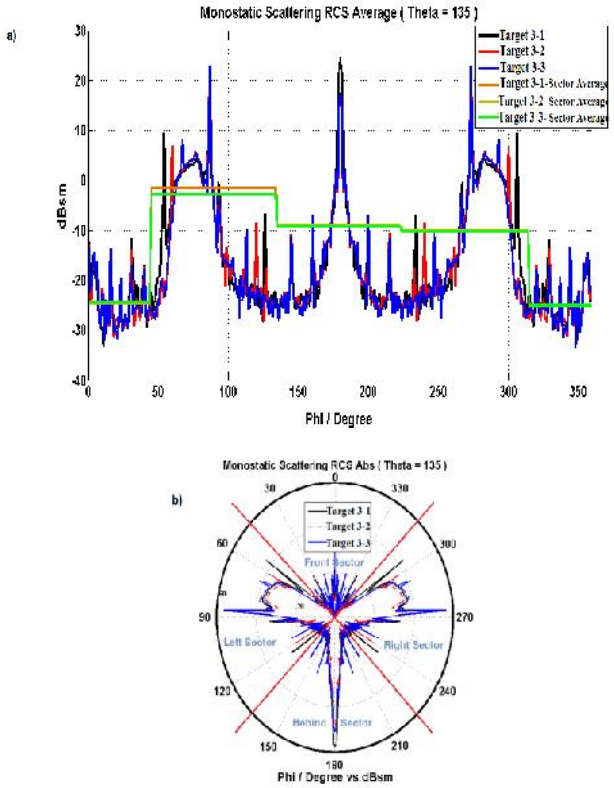

Fig. 7.a) The RCS average value of target geometry 3 over X-Band. b) Normalized RCS to maximum value (polar mode)

Table 2 shows the RCS average value of geometry 3 over X-band and average over four angular sectors, we can find from Table1, the best average RCS value is by using target 3-3.

Table2: The RCS average value of Geometry2 over X-Band and over four angular sectors ($\theta = 135^0$).

Geometry 3	**RCS Average (dBsm) for $\theta = 135^0$**				
	Total average	**φ = $315{:}45^0$ Front sector**	**φ = $45{:}135^0$ Left sector**	**φ = $135{:}225^0$ Behind sector**	**φ = $225{:}315^0$ Right sector**
Target 3-1	**-16.21**	**-24.33**	**-1.52**	**-9.09**	**-10.21**
Target 3-2	**-16.85**	**-24.90**	**-2.69**	**-9.09**	**-10.12**
Target 3-3	**-17.04**	**-25.87**	**-2.80**	**-9.23**	**-10.33**

3.4 Target Geometry 4

Target geometry 4 consists of target geometry 3 and Tail. There are many shapes and types of tail but we select three type, two consist of two parts and other one part so we will get three UAV types, Figure. 10 show those three types.

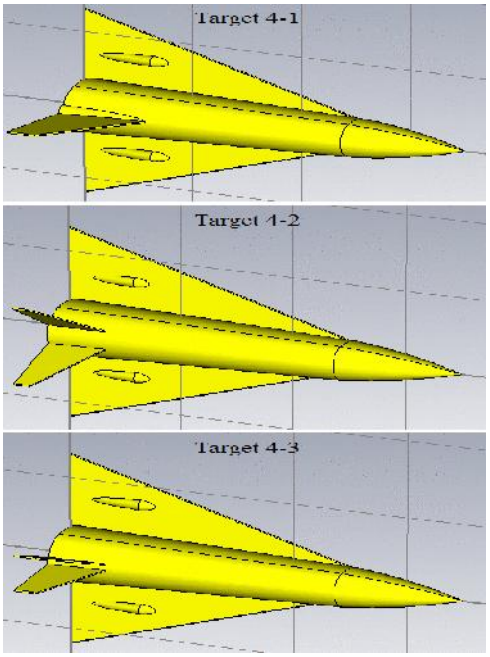

Fig. 8. Target geometry 4

Figure. 9 shows the RCS average value of target geometry 3 over X-band .The RCS computations were performed at: $\theta = 135^0$ and $\varphi = 0: 360^0$ with 1^0 steps

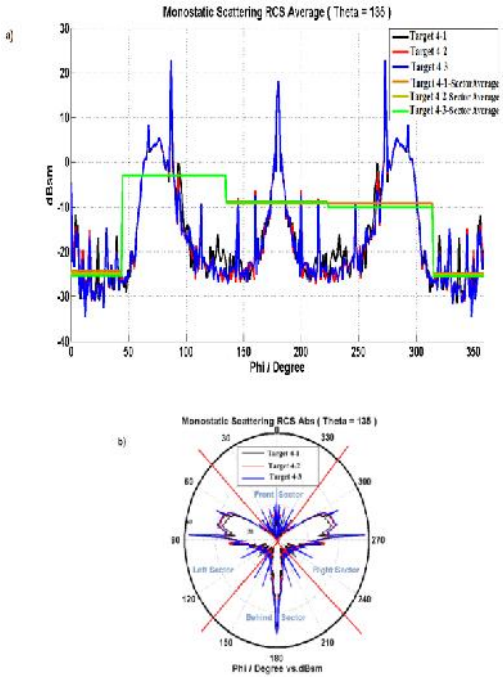

Fig. 9. a) Average value of radar cross section at four angular sectors geometry4 over X-Band, b) Normalized RCS to maximum value (polar mode)

Table 3 shows the RCS average value of geometry 4 over X-Band and average over four angular sectors, we can find from Table3, the best average RCS value is by using target 3-4.

Table 3: The RCS average value of Geometry 4 over X-Band and over four angular sectors ($\theta = 135^0$).

Geometry 4	RCS Average (dBsm) for $\theta = 135^0$				
	Total average	φ = $315:45^0$ Front sector	φ = $45:135^0$ Left sector	φ = $135:225^0$ Behind sector	φ = $225:315^0$ Right sector
Target 4-1	-16.60	24.72	-2.22	-9.14	-9.23
Target 4-2	-16.33	-24.52	-2.90	-8.98	-10.12
Target 4-3	-17.1	-25.50	-2.85	-9.20	-10.16

4. Geometry 4 Compares the Results with Reference

Reference: it consists of nose (ogive), wing (SemDelta) and tail with one part.

Target 4-3: this type is final model, it consists of nose (ogive), wing (Delta) and tail with two parts.

Figure.. 10 shows the RCS average value of target geometry 4 (Target 4-3) and geometry reference over X- band .The RCS computations were performed at:

$\theta = 135$ and $\varphi = 0: 360^0$ with 1^0 step.

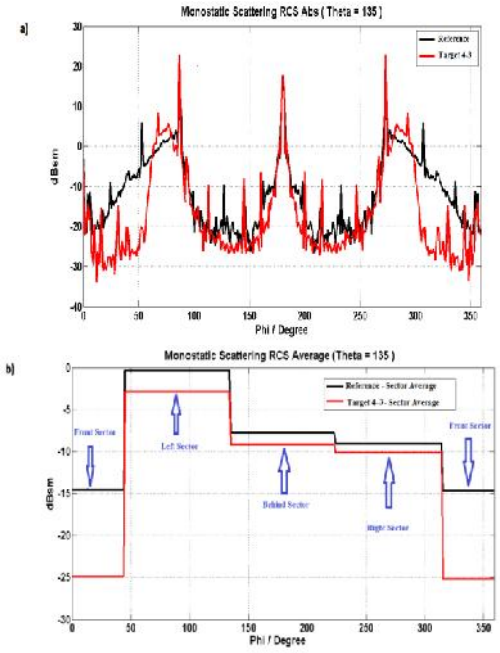

Fig. 10. a) The RCS average value of target geometry 4 (Target 4-3) and geometry reference over X-Band, b) The RCS average value of target geometry 4 (Target 4-3) and geometry reference over X-Band and over four angle sectors.

Table-4 shows the RCS average value of geometry4 (Target 4-3) and geometry reference over X-band and average over four angular sectors.

Table4: The RCS average value over X-Band and over four angular sectors ($\theta = 135^0$)

Model	**RCS Average (dBsm) $\theta = 135^0$**				
	Total average	**φ = $315{:}45^0$ Front sector**	**φ = $45{:}135^0$ Left sector**	**φ = $135{:}225^0$ Behind sector**	**φ = $225{:}315^0$ Right sector**
Reference	**-11.9**	**-14.57**	**-0.34**	**-7.78**	**-9.07**
Target 4-3	**-17.1**	**-25.06**	**-2.85**	**-9.20**	**-10.2**

The simulation results give the same results that the target 4-3 give the RCS average value (Target 4-3 the final model we got in this study) reduced as much as -5.12dBsm then geometry reference.

5. CONCLUSION

In this paper number of steps is presented to reduce RCS of complex aerial target by building optimum design, which reduces RCS.

Generally the correct determination of the RCS of an object is rather difficult task, so in this paper we present one simulation method that depends on CST software over X-band. The comparison between RCS simulation reference results and geometry 4 (Target 4-3) results show RCS average using the technique of shaping is reduced In each sector so that the sector left angular size -2.51dBsm, the sector behind to size -1.42dBsm, the right sector to size -1.13dBsm and radar cross section of a front that moved as detection by enemy radar systems is important, cut to size -10.49dBsm reference to the UAV.

REFERENCES

[1] D. C. Jenn, Radar and Laser Cross Section Engineering, 2nd ed, AIAA education series, 2005.

[2] N. N. Youssef, "**Radar Cross Section of Complex Target**, " IEEE, VOL.77, NO. 5, May 1989.

[3] G. A. and C. Sr, " **The descriptive geometry of nose cone**, " 1996.

[4] I. M. M r n, M. A. Alve , G. G. Pe xo o , nd M. C. Rezende, "**Radar Cross Section on Measurement and Simulations of a Model Airplane in the X-b nd**, " PIERS Onl ne, Vol. 5, No. 4, 2009..

[5] CST, EM Software & Systems, Available: http://www.cst.com. Accessed JUNE, 2011.

[6] L. Sevgi, "**Radar Cross Section (RCS) prediction techniques: from high frequency asymptotic to numerical simulations**, " University Zeamet Sok., No.2 , Acıb dem Turkey 2 4..

[7] J. M. Rius, M. Ferrando, and L. Jofre, "**High-Frequency RCS of Complex Radar Targets in Real-Time**, " IEEE, VOL. 41, NO. 9, September 1993.

[8] Chinn, S.S.; Missile Configuration Design, McGraw-Hill Book Co., Inc, New York, Copyright 1961.

[9] Knott, E. F., J. F. Schaeffer, and M. T. Tuley, Radar Cross Section Measurements, Artech House Inc, Norwood, 1993.

[10] "**IEEE Standard Definitions for Terms for Antennas,**" IEEE Trans. On Antennas and Propagation, vol. AP-37, pp. 956-966, June 1989.